Automatic CNC Program Generation From Range Data

Dietrich Paulus[1], Karl–Heinz Kunzelmann[2],
Stefan Küppers [1], Heinrich Niemann[1,3], Matthias Wolf[3]

1: Universität Erlangen–Nürnberg
Lehrstuhl für Mustererkennung (Informatik 5),
Martensstraße 3, D–91058 Erlangen

2: Poliklinik für Zahnerhaltung und Parodontologie München
Ludwig–Maximilians–Universität München
Goethestraße 70, 80336 München

3: Bayerisches Forschungszentrum für Wissensbasierte Systeme
(FORWISS) – Forschungsgruppe Wissensverarbeitung
Am Weichselgarten 7, 91058 Erlangen

paulus@informatik.uni-erlangen.de
Karl-Heinz.Kunzelmann@Dent.MED.Uni-Muenchen.de

Appeared in
Conference Proceedings
Int. Conference on Recent Advances in Mechatronics,
Istanbul, August 1995

D. Paulus, K.-H. Kunzelmann, H. Niemann, M. Wolf: *Automatic CNC Program Generation From Range Data*, in O. Kaynak, M. Özkan, N. Bekiroglu, I. Tunay (Hrsg.): *Int. Conference on Recent Advances in Mechatronics*, Bd. 1, Istanbul, 1995, S. 230–237.

Automatic CNC Program Generation From Range Data

Dietrich Paulus[1], Karl–Heinz Kunzelmann[2],
Stefan Küppers [1], Heinrich Niemann[1,3], Matthias Wolf[3]

1: Universität Erlangen–Nürnberg
Lehrstuhl für Mustererkennung (Informatik 5),
Martensstraße 3, D–91058 Erlangen

2: Poliklinik für Zahnerhaltung und Parodontologie München
Ludwig–Maximilians–Universität München
Goethestraße 70, 80336 München

3: Bayerisches Forschungszentrum für Wissensbasierte Systeme
(FORWISS) – Forschungsgruppe Wissensverarbeitung
Am Weichselgarten 7, 91058 Erlangen

paulus@informatik.uni-erlangen.de
Karl-Heinz.Kunzelmann@Dent.MED.Uni-Muenchen.de

Abstract In this paper we report on a successful cooperation of three institutes in the areas of applied image analysis for dentistry.

In the application, range images recorded with a high–precision laser sensor are the input to image analysis. Surface patches of varying size and type are fitted to the data (Sect. 2). Various views from known positions are used to fuse the computed patches to complete 3D model with the accuracy required for medical applications. The result of the computation is put in a common CAD format suited for automatic manufacturing of ceramic tooth inlays.

The system has also been applied to other technical objects, as we show by an example.

1 INTRODUCTION

We describe a system which captures images of a 3D object from several directions with a high–precision laser sensor. The system was implemented in [10]. These images — together with the transformation data of the capturing device — are used to create a 3D surface map of the object. Surface patches of arbitrary order are fitted to the range data and the object is transformed to normal position. After resampling, the images are matched using maximum elevations and derivatives at these locations. A 3D description of the surface is created which is again approximated by patches. These parameterized functions are converted to VDA–FS format ([7], see Sect. 2.1) which is a CAD format used for industrial production, allowing for immediate reproduction of the object by a CNC machine. The sequence of processing steps is shown in Figure 1.

The major application of this system is dentistry. To overcome material variations the use of high quality materials processed under standardized criteria is mandatory. Milling dental restorations from preshaped ceramic blocks using CAD/CAM technology not only guarantees high material qualities but allows also quick and cheap production of these restorations.

A system for reconstruction of tooth data is described in [12]; reference points for matching have to be marked by an operator. Matching and data fusion without human interaction will speed up automatic milling.

Already existing industrial devices measure cavities prepared during the treatment of caries to restore the decayed tooth structure with inlays or crowns (e.g. the CEREC^{R}system, [11]). The 3D model of the object to reconstruct the tooth defects is generated interactively by a dentist. This procedure is prone to operator errors and requires high

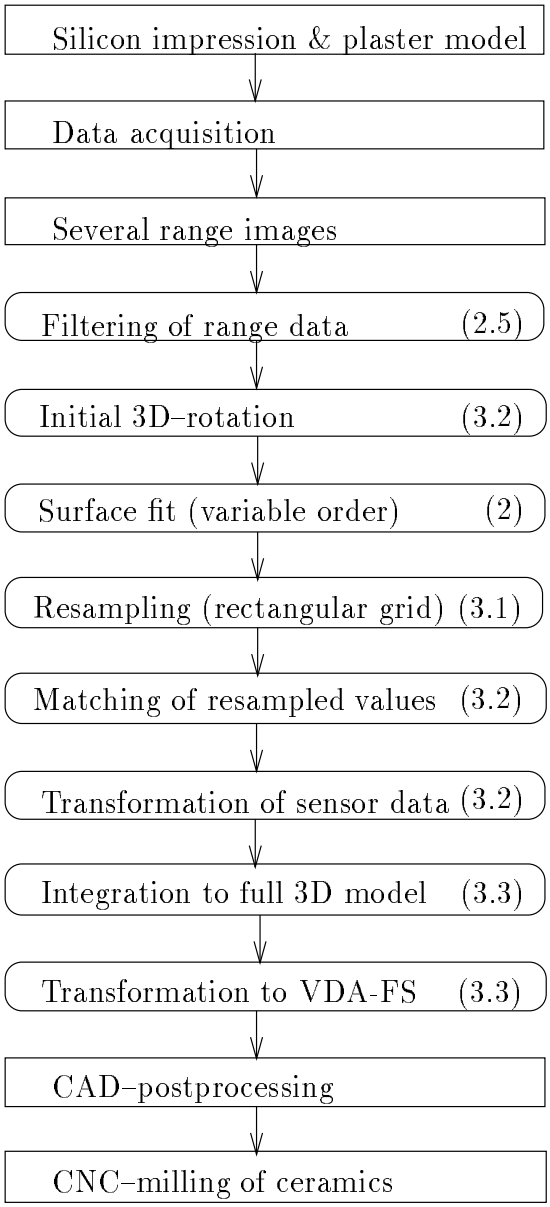

Figure 1: Strategy: steps in rectangular boxes were implemented in [8, 5], round boxes are described in this paper based on [10], section numbers in parentheses.

training skills of the operator. Currently, no information concerning the chewing surface of the tooth can be considered resulting in the need to manually adjust the surface to the reconstruction to the opposing tooth surface, which has to be done with high precision and is not only time consuming but also rather unpleasant to the patient. To improve processing speed the commercial systems interpolate the surface inside the cavity reducing the accuracy of fit to an average of 150μ at best. The remaining gap has to be closed with low viscosity luting materials with reduced mechanical properties which decrease the life–time of the reconstructions.

Our approach shows how to obtain high–precision 3D CAD models of inlay or crown restorations. In order to improve the accuracy of the three dimensional shape measurement and to overcome the problem of shading within the object's surface the tooth surface without a reconstruction is measured in a divisional approach. A plaster model of the prepared tooth is mounted on an actor (computer controlled gonio stage) and measured at different tilt angles and rotations around the vertical axis of the tooth with a high–precision laser sensor using the triangulation principle. By obtaining the profile of a light knife at the speed of a video frame of a CCD chip the 3D data are acquired within a few seconds. After measuring the prepared tooth a dental technician reconstructs the tooth surface with wax adjusting it precisely to the opposing tooth. The partial data sets are combined to one single 3D data set using the movement information of the actor refined by matching the partial information using overlapping areas. This two–stage process is necessary because the exact position of the rotation axes of the *dies* is not known due to large variations in tooth geometries. The process of fabricating die models from plaster out of silicon impressions of the teeth and to reconstruct the defect with wax is part of the daily dental routine and is performed within a few minutes.

For the dental application, we compare the results of 2^{nd} and 3^{rd} order surface approximations and give quantitative results of the approximations.

A new test criterion is introduced and used to select only those points from the data set for approximation which are useful for the reconstruction. Thereby, even rapid changes in depth can be modelled with high accuracy. The resulting inlay can be manufactured in ceramics by a CNC machine. The sensor accuracy is 10μ; the maximum error for approximation is 4μ. Since 50μ are regarded sufficient in dentistry, this approach is more than adequate.

The VDA–FS format is mainly used in automobile industry. We give an outlook how our system can be used for larger objects, and how the senor will be guided to find concave and occluded areas automatically.

2 SURFACE FITTING

2.1 Motivation

Range images f_{ij} $(0 \leq i < M, 0 \leq j < N)$ represent objects by discrete values at discrete locations:

$$f_{ij} = f(x_0 + i\,\Delta x,\; y_0 + j\,\Delta y). \qquad (1)$$

Arithmetic operations on range images like rotation, calculation of derivates, curvatures an so forth, have to deal with the problem of interpolating to values between these discrete locations. This should be done in a fast way and with minimum error. For example, after rotation of such data the discretization grid will no longer be rectangular and the exact values could not be stored in the Form of (1). A parametric surface fit of the range data facilitates an analytic calculation of all desired properties and also requires less storage.

In the dental application, the complete 3D model has to be manufactured in ceramics using CNC machines. These devices can be controlled via standardized interfaces; one of them is the surface model by "Verein der Automobilindustrie" which is commonly used (VDA–FS [7]). General parametric polynomials are used for surface representation with p and q as the maximum order of u and v:

$$\begin{aligned} X(u,v) &= \sum_{k=0}^{q}\sum_{j=0}^{p} a_{jk} u^j v^k \\ Y(u,v) &= \sum_{k=0}^{q}\sum_{j=0}^{p} b_{jk} u^j v^k \qquad (2) \\ Z(u,v) &= \sum_{k=0}^{q}\sum_{j=0}^{p} c_{jk} u^j v^k. \end{aligned}$$

In [1] the following bivariate polynomials are used with great success for 3D object segmentation in range images

$$g(n, \boldsymbol{a}, u, v) = \sum_{i+j \leq n} c_{ij} x^i y^j \quad (n \leq 4), \qquad (3)$$

where g approximates the range values at x, y coordinates; x and y are computed from the values f_{ij} by a shift to the origin and scaling. Other approaches to surface approximation can be found in e.g. [2]. Multiple views are combined to surfaces in e.g. [3].

Generally, range data have to be clustered to surface patches of varying size which are then approximated by these polynomials. We show that we can fulfill the requirements in dentistry and approximate very fine structures, which can be found at molars, with a much smaller fit–error than the desired 50μ. These results can be represented in VDA–FS format and passed to a CNC machine to build the ceramic reconstruction of a tooth defect.

2.2 Algorithm

Our algorithm for surface approximation by a finite number of surface patches has four input arguments: a set of 3D coordinates of possibly scattered points, the size of the rectangular area to be approximated (p_x, p_y), the maximal distance ξ in z direction, and the maximal tolerable approximation error δ; i.e. range data has not to be provided in a rectangular grid as in (Eq. 1).

The size of the patch has to be chosen in such a way that a reasonable number of data points can be found inside, to allow for a stable estimation of the surface parameters. If – on the other hand – the size of the patch is large and if many points can be found inside this area, the approximation error for this patch will be large.

In our application the maximal ξ has to be chosen for each tooth separately as well as δ. For molars with a patch size of $p_x = p_y = 100\mu$ a value of $\delta = 4\mu$ turned out to be a good choice.

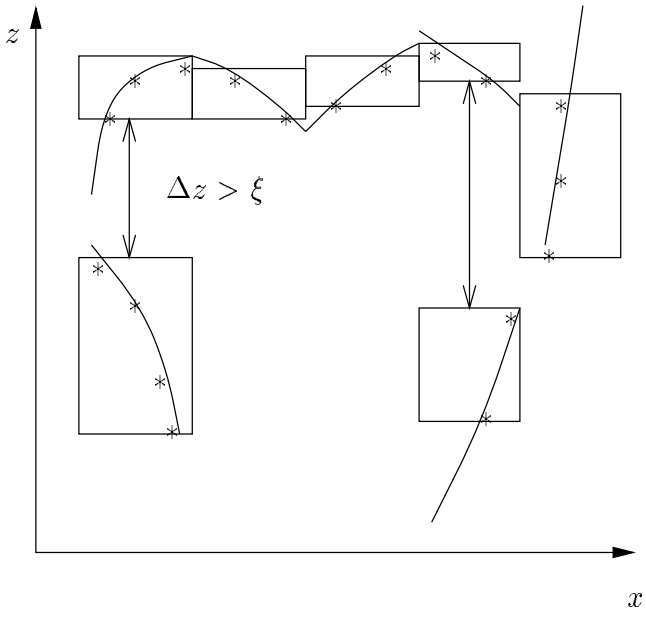

Figure 2: Patch border without smoothing

After sorting of the range data into cubes depending on the choice of ξ, patches are computed for the values in these volumes. Depending on the number of samples inside of a cube, bivariate polynomials of varying order are approximated using least square error fitting. This basic idea is extended in the following section.

2.3 Smoothing

In the first step we divide the object space into rectangular areas and calculate a parametric description from the 3D values inside these areas using (3). The resulting neighboring patches differ at the borders in their orientation considerably (see Figure 2).

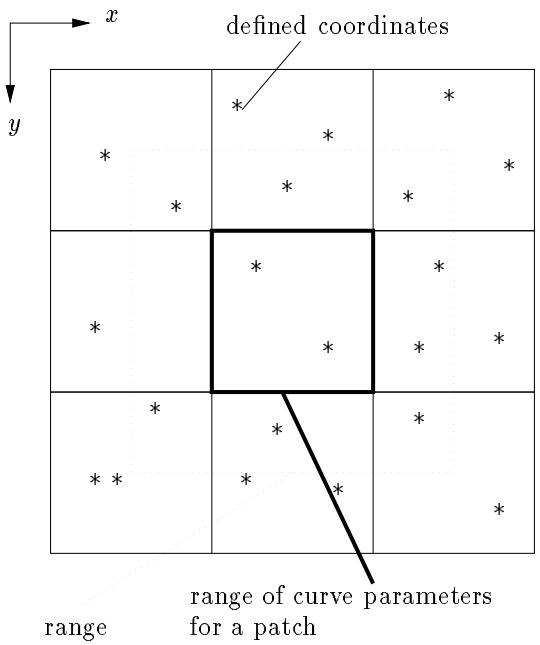

Figure 3: Range for smoothing

In order to smooth transition between neighboring patches, approximation of range values considers the sample values in parts of the adjacent volumes as shown in Figure 3. In addition to smoothing, this also increases the number of sample points for the approximation (Figure 4). Thereby, a higher order polynomial or a smaller patch size can be chosen which can represent even small details in the range image. Results of this extension can be seen in Figure 7.

2.4 Adaptive Refinement

The algorithm described so far works fine inside an object. However, at object borders no neighboring

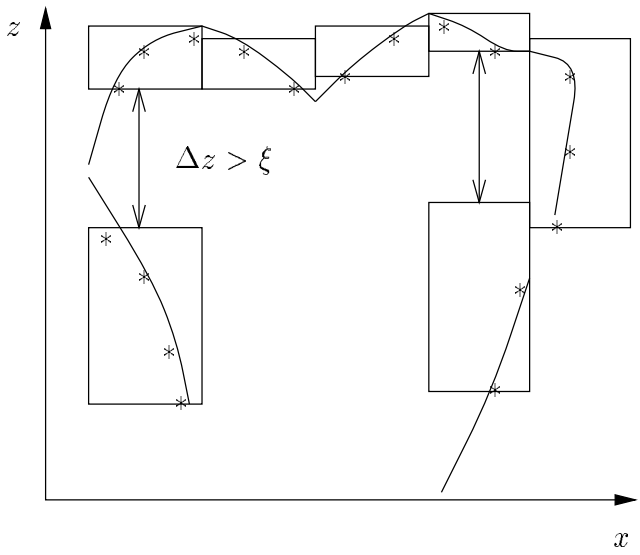

Figure 4: Patch border with smoothing

range data can be taken into account and borders are not rectangular in general. The solution is to reduce the patch size in these areas by splitting. Reduced patches containing no range data are assumed to be outside the object and discarded.

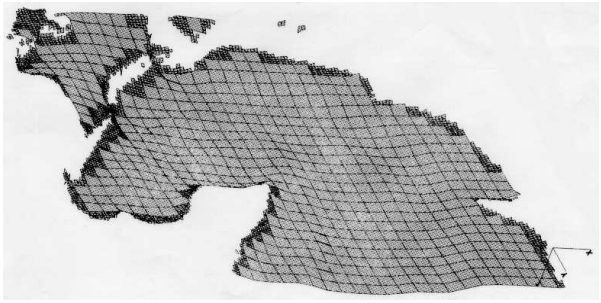

Figure 5: Surface approximation of a chess knight with varying patch size

As shown in Figure 5, object borders are clearly separated from the background. Small patches in this application have a size of $70\mu^2$ and large patches are $350\mu^2$. Even in the middle of the figure, large patches could be used.

2.5 Elimination of Noise

Various tests for plausibility of the range information are used to eliminate the few remaining noisy samples, mainly at corners. If the distribution of range

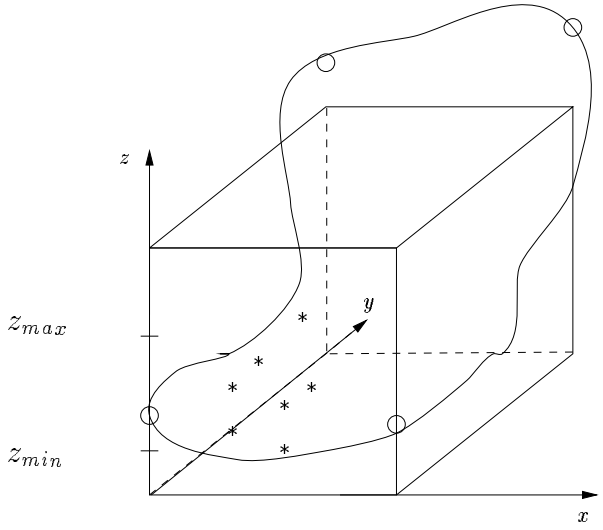

Figure 6: Elimination of noise

data only uses a small part of the cubic surface definition sphere (as shown in Figure 6), the direction of the calculated surface in the rest is nearly random, but in the direction of the outer 3D data. The "corner test" (Figure 6) uses the values at the limits of the range. If the actual range values at the borders of the definition sphere of a patch is considerably (using a threshold) larger than maximal z–coordinate value or smaller than the minimum value, the patch is marked undefined. Only in rare cases this leads to elimination of correct values close to very steep descents.

If the reduced patch size is too small, this area is marked undefined as well. The remaining patches approximate the surface with the required accuracy.

2.6 Results

The following function was used for judging the approximation error in a patch with L 3D values, calculating the differences between sensor data z_i and computed surface values $f(x_i, y_i)$:

$$ {}^n f_{max} = \max\{|z_i - f(x_i, y_i)|, 1 \le i \le L\} \quad (4) $$

$$ {}^n \bar{f} = \frac{1}{L} \sum_{i=1}^{L} |z_i - f(x_i, y_i)| \quad (5) $$

$$ {}^n \bar{f}_\delta = \frac{1}{P} \sum_{i=1}^{P} |z_i - f(x_i, y_i)| \quad (6) $$

The error value ${}^n f_{max}$ is the maximal difference of a range value to the approximating polynomial surface of degree n, the number ${}^n \bar{f}$ is the mean difference of all range values and ${}^n \bar{f}_\delta$ is the mean difference for the P range values which lay in patches with a surface–fit–error smaller than δ. Table 1 lists results for six teeth where in (6) a δ of 4μ is chosen; the small differences between ${}^n \bar{f}_\delta$ and ${}^n \bar{f}$ show that the occurrence of great errors is very rare, and the limit of 4μ is much smaller than the sensor noise of 10μ. Large values of ${}^n f_{max}$ can be found only at boarders of the object and could be eliminated by the corner test as can be seen from the small value of ${}^n \bar{f}$.

The best results were obtained with polynomials of degree 3 and 4, whereby the parameter range was $120\mu^2$. The mean approximation error was 2.4μ. The error reduction by the use of the restrictions in Sect. 2 is obvious from the differences of ${}^n \bar{f}$ and ${}^n \bar{f}_\delta$. Computation time however grows quadratically with the number of parameters. On an 80486–Intel–PC (Linux), approximation for first order is approx. 1 minute, second order 3 minutes, third order 7 minutes and fourth order 15 minutes. Figure 7 shows some results on real teeth. The calculated surface was resampled to range images.

3 3D MODEL

In a single sensor range image you get the data of one view of an object. So the range data from several views are now fused to a complete 3D model of an object. The fusion and matching is performed on resampled range data (Sect. 3.1, 3.2). The final 3D model is again represented as parametric surface patches (Sect. 3.3).

3.1 Resampling

First a matching of the different views is performed to calculate the six location parameters, then all views will be rotated and translated following these parameters, so that the 3D values of all views can build a complete model of the object. For this matching step, data recorded from two views are transformed into each other minimizing the distance between the surfaces (Sect. 3.2). This is done with a system described in [5] which requires input data sampled in a rectangular grid. Range data are thus resampled from the computed surface patches of the single views.

Tooth	${}^1f_{max}$	${}^1\bar{f}$	${}^1\bar{f}_\delta$	${}^2f_{max}$	${}^2\bar{f}$	${}^2\bar{f}_\delta$	${}^3f_{max}$	${}^3\bar{f}$	${}^3\bar{f}_\delta$	${}^4f_{max}$	${}^4\bar{f}$	${}^4\bar{f}_\delta$
z0	4303.7	5.6	3.2	2824.7	3.5	2.7	54.5	2.6	2.5	48.6	2.5	2.4
z1	2194.0	5.1	3.2	356.9	3.1	2.7	68.2	2.7	2.5	25.8	2.5	2.4
z2	9127.8	7.7	3.0	22200.1	12.3	2.5	5606.0	5.7	2.3	224.0	3.2	2.3
z3	1322.1	7.8	3.0	10120.1	9.1	2.6	1971.5	3.7	2.4	698.1	5.2	2.2
z4	61.1	5.1	3.0	43.1	3.5	2.6	37.5	3.1	2.4	245.0	3.0	2.4
z5	46.3	4.8	3.1	34.3	3.1	2.7	14.1	2.6	2.4	351.1	4.2	2.5

Table 1: Approximation error for six teeth

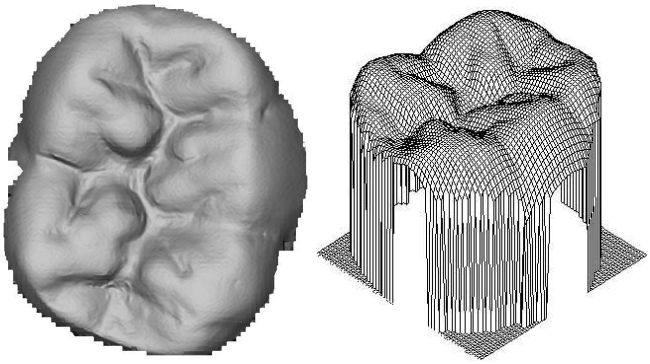

(a) Varying order approximation (grey shading)

(b) Varying order approximation(mesh plot)

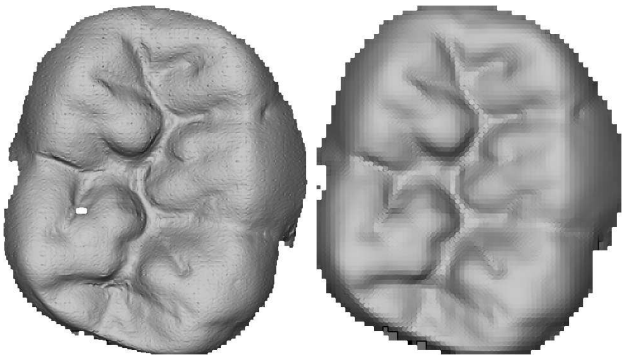

(c) Varying order approximation without smoothing

(d) First order approximation

Figure 7: Tooth surface

3.2 Matching

One view is chosen as a model of the object. All other views are then matched against this model. Matching is done using a Levenberg–Marquard–algorithm. Distance is computed pixelwise for all known corresponding points in model and object. The algorithm minimizes the mean distance of the surfaces.

The algorithm works well, if translational distance of the views is smaller than 10 % of the object length an the rotational distance is smaller than five degree per axis. To fulfill this rule, a norming step of the object position must be performed. First, range data is rotated around initial angels which are input from the human operator operating the sensor; a result is shown in Figure 8. Afterwards all 3D values are shifted, with the result that the shortest defined value at each axis begin at zero. Matching of teeth, in addition, only uses the upper surface, since the sides are different in each view and have only little surface structure. A polynomial surface is calculated from these normalized data with the effect of smoothing, and in this application, this simplifies the matching process.

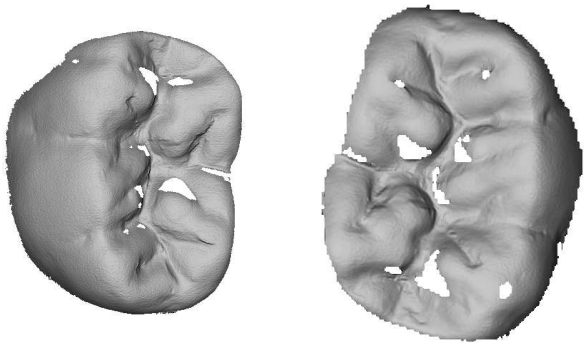

(a) Original data

(b) After initial rotation

Figure 8: Initial rotation for matching

3.3 Fusion

The normalized and matched views are now integrated to a complete model, using the transformation parameters computed in Sect. 3.2. This is again approximated by parametric surfaces. The results of

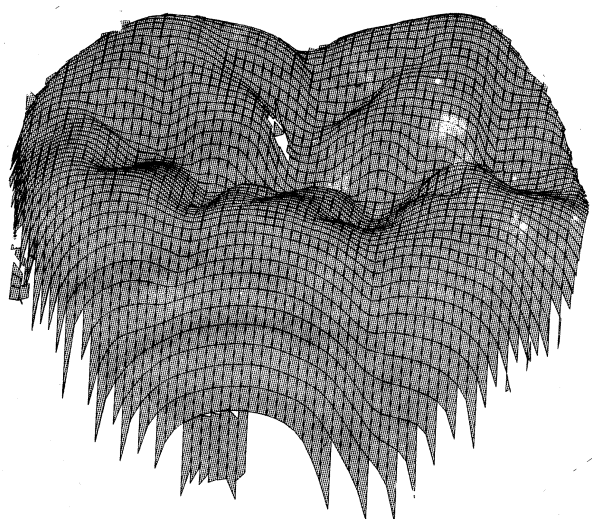

Figure 9: Finite element graphics

surface approximation are converted to VDA–FS and then passed to a separate graphics program. This program interprets the VDA–FS data, produces a finite element description, and visualizes the finite elements. Figure 9 shows the result of such a reconstruction for the tooth shown in Figure 8.

The images in Figure 10 show different views of one tooth with cavities which have sharp edges and ridges, as they are common in works for surfaces with sharp edges and ridges, as they are common in dentistry after treating the caries and prepared cavities. The white spots inside the hole are occluded areas not visible to the sensor.

The reconstructed result in 11 proves that the whole sequence of processing steps is operational. The range occluded in all four views in Figure 10 is missing in the reconstruction (on the right side, and on the front, see also the white areas in Figure 12). This could be filled with interpolated values. On the left ridge, small errors resulting from the high order of the polynomials can be found. If the dentist knows about this property of the system, appropriate preparation as on the right side can avoid this behavior.

4 EFFICIENCY

Original range data were recorded with 512^2 floating point values. Usually, 10 images were used for the construction of a complete 3D model. A typical surface reconstruction of 3000 surface patches requires approx. 540 Kbyte storage, which is considerably smaller than the complete 3D data (10 Mbyte).

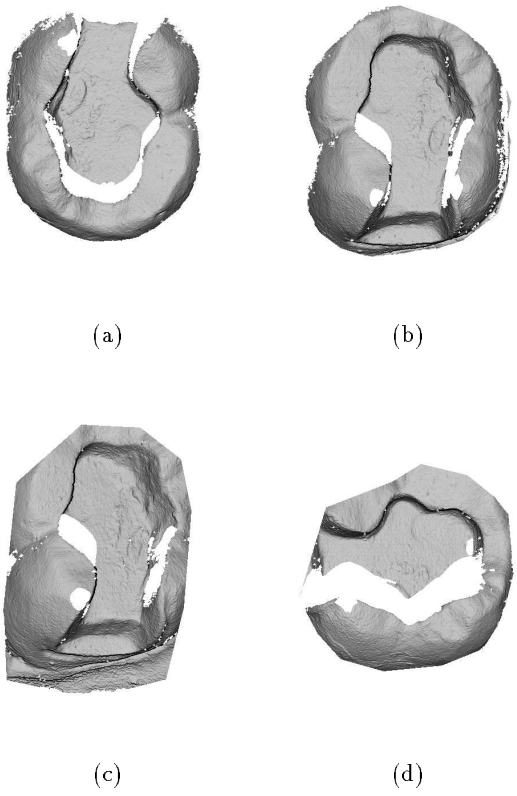

Figure 10: Parts of a tooth with cavity

The time needed on a PC (Intel 80486/33) to build

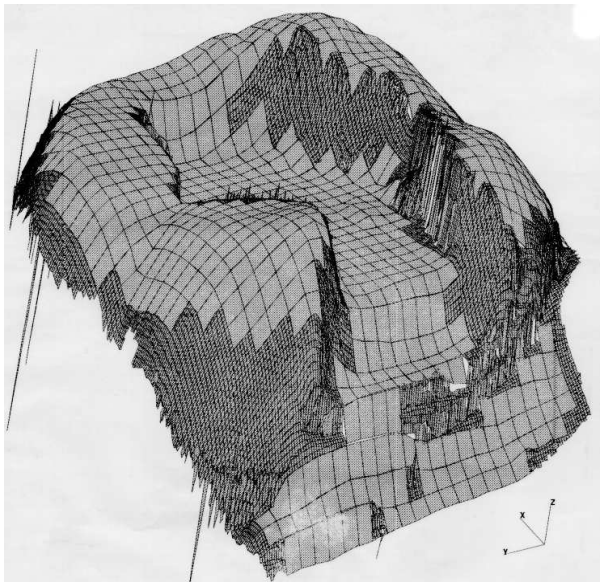

Figure 11: Finite element graphics

a complete model from the four different range images in Figure 10 is two to 20 minutes, depending on the polynomial order, and other known applications need this time only to calculate one parametric surface from one range image. The computing time depends linearly on the number of 3D values.

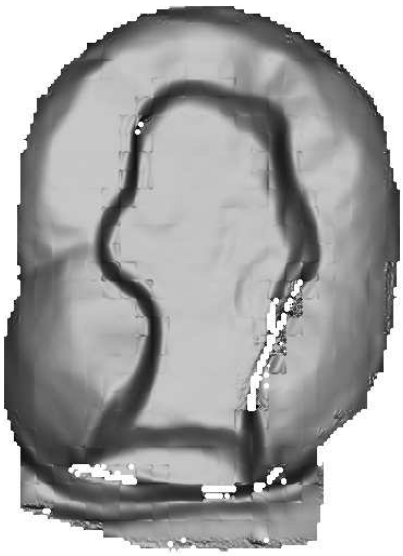

Figure 12: Fused views (from images in Figure 10)

5 RESULTS

Model matching of pre–processed range images could be done with a mean error of about 10μ; this is close to the sensor noise. Fusion of surfaces and matching turned out to be stable. Through the combination of the different views most shadowing areas could be eliminated (see Figure 10 and 11). A mean filter in small surface areas of $50\mu^2$ was tested for noise reduction. This was not required for the final matching and did not change the quality of the results. It reduced however the time for computation.

References

[1] Besl, P.: *Surfaces in Range Image Understanding*. Springer–Verlag New York 1988.

[2] F. Solina, R. Bajcsy: *Recovery of parametric models from range images, IEEE Trans. on Pattern Analysis and Machine Intelligence*, Bd. 12, Nr. 2, 1990, S. 131–147.

[3] M. Sourcy, D. Laurendeau: *Generating non-redundant surface representations of 3D objects using multiple range views*, in *Proceedings of the* 11^{th} *International Conference on Pattern Recognition (ICPR)*, IEEE Computer Society Press, The Hague, Netherlands, August 1992, S. 198–200.

[4] Hofmann, G.R.: *Imaging, Bildverarbeitung und Bildkommunikation*. Springer Verlag 1993.

[5] Neugebauer, P.: *Feinjustierung von Tiefenbildern zur Vermessung von kleinen Verformungen*. Diploma thesis Lehrstuhl für Mustererkennung (Informatik 5), Universität Erlangen–Nürnberg 1991.

[6] Niemann, H.: *Pattern Analysis and Understanding*. Springer–Verlag, Berlin, 1989.

[7] Editor: DIN:Deutesches Institut für Normung e.V. *DIN-Taschenbuch 200 /CNC-Maschinen /Num. Steuerung*. Beuth Berlin, Köln 1992

[8] M. Wolf: *Merkmalsextraktion für Kauflächen*, Diploma thesis, Lehrstuhl für Mustererkennung (Informatik 5), Universität Erlangen–Nürnberg, Erlangen, 1994.

[9] Krämer, N., Kunzelmann, K.–H., Pelka, M., Occlusal three–dimensional measurements as prerequisite for tool shape–optimization in CAD–CAM–restaurations, 31^{st} annual meeting CED/IADR, Lyon, 1993 (Poster)

[10] S. Küppers: *Generierung eines 3D Zahnmodels aus 2,5D-Sensordaten*, Diploma thesis, Lehrstuhl für Mustererkennung (Informatik 5), Universität Erlangen–Nürnberg, Erlangen, 1995.

[11] W. H. Mörmann, M. Brandestini: *Die CEREC Computer Reconstruction: Inlays, Onlays und Veneers*, Quintessenz Verlags-GmbH, Berlin, 1989.

[12] T. Ozaki, E. Kanazawa, M. Sekikawa, J. Akai: *Three–dimensional measurements of the occlusal surface of the upper molars in Australian Aboriginals*, *Australian Dental Journal*, Vol. 32(4), 1987, p. 263–269.